

Optimum Photoluminescence Excitation and Recharging Cycle of Single Nitrogen-Vacancy Centers in Ultrapure Diamond

K. Beha,¹ A. Batalov,^{1,*} N. B. Manson,² R. Bratschitsch,^{1,†} and A. Leitenstorfer¹

¹*Department of Physics and Center for Applied Photonics, University of Konstanz, D-78457 Konstanz, Germany*

²*Laser Physics Centre, Australian National University, Canberra, ACT 0200, Australia*

(Received 11 September 2011; published 30 August 2012)

Important features in the spectral and temporal photoluminescence excitation of single nitrogen-vacancy (NV) centers in diamond are reported at conditions relevant for quantum applications. Bidirectional switching occurs between the neutral (NV^0) and negatively charged (NV^-) states. Luminescence of NV^- is most efficiently triggered at a wavelength of 575 nm which ensures optimum excitation and recharging of NV^0 . The dark state of NV^- is identified as NV^0 . A narrow resonance is observed in the excitation spectra at 521 nm, which mediates efficient conversion to NV^0 .

DOI: 10.1103/PhysRevLett.109.097404

PACS numbers: 78.55.Ap, 42.62.Fi, 61.72.jn, 81.05.ug

Recently, the nitrogen-vacancy (NV) defect center in diamond had attracted rapidly growing interest due to its long spin coherence times together with the possibility of optical spin initialization and readout [1]. It is promising for various aspects of quantum-information processing [2–4] and magnetometry on the nanoscale [5,6]. Because of their structural stability, NV centers represent robust single-photon sources [7,8] which have already found commercial applications. One important goal in this context is the generation of indistinguishable single photons [9], which are essential for long-distance entanglement protocols in quantum technology [10]. Currently, spectral jumps and diffusion of emission lines under nonresonant excitation are limiting factors [11]. Another drawback is the dark state of NV^- , where it spends a considerable amount of time [12]. Interestingly, there are no systematic studies of the photoluminescence (PL) emission of single NV centers depending on excitation wavelength.

In this Letter, we present photoluminescence excitation (PLE) spectra and time-resolved emission measurements of single NV centers performed in the temperature range between 10 and 300 K. The excitation wavelength λ_{exc} is varied continuously over the entire visible spectrum and a sharp maximum of optimum PLE from NV^- is found at $\lambda_{\text{exc}} = 575$ nm. The nature of the dark state is elucidated and an efficient way to predominantly keep the center in its neutral form NV^0 is discovered. Our findings represent important cornerstones for a detailed understanding of the operation of NV centers.

We work with an ultrapure specimen of diamond (concentration of nitrogen atoms <5 ppb, separation between single NV centers ~ 10 μm) grown by chemical vapor deposition. A hemispherical solid immersion lens [13] (cubic zirconia, diameter 2 mm) is placed on the polished surface of the sample to enhance PL collection. An objective lens for confocal excitation and collection of emitted photons (with a numerical aperture of 0.75) is mounted in front of the window

of a liquid-helium flow cryostat. A widely tunable Er: fiber laser system [14] serves as a pump source in the wavelength range between 440 and 700 nm. Pulses of duration of 1 ps and a spectral bandwidth of 1 nm at the fundamental repetition rate of 40 MHz or its subharmonics are provided in this way. Alternatively, three continuous-wave (cw) lasers are available emitting at 532, 488, and 406 nm. The PL emission from single NV centers is analyzed with an EMCCD array placed behind a grating monochromator. A Hanbury-Brown–Twiss setup [7] and a single avalanche photodiode allow for time-resolved measurements.

We first ensure that a single NV center is studied via the absence of a central peak at $\tau = 0$ in the photon autocorrelation function $g^{(2)}(\tau)$ [7]. An example under excitation with an interpulse distance of 75 ns at $\lambda_{\text{exc}} = 532$ nm and collection with a long pass filter at 640 nm is depicted in the inset of Fig. 1(a). Subsequently, any influence of pulsed versus cw excitation on the PL spectra was checked. No difference was found for the entire range of intensities used in this study when comparing the spectral emission triggered by the cw sources at $\lambda_{\text{exc}} = 488$ and 532 nm with results using the fiber laser tuned to the same wavelengths. PL spectra obtained by pumping at 521 and 550 nm are shown in Figs. 1(a) and 1(b). Generally, a background has been accumulated independently at a position displaced by 2 μm from the NV center and subtracted. The PL emission contains a superposition of signatures of the negatively charged NV^- and the neutral defect NV^0 . Both components consist of a sharp zero phonon line (ZPL, at 637 nm for NV^- and at 575 nm for NV^0) and associated phonon sidebands (PSB) [15]. The PL contribution from each charge state depends strongly on excitation wavelength but is similar for every single defect. None of the centers are found in a pure charge state.

For lifetime measurements, time-resolved PL is accumulated in the spectral window from 575 to 630 nm (from 660 to 800 nm) for NV^0 (NV^-). In both cases the traces fit well to a monoexponential decay [inset in Fig. 1(b)].

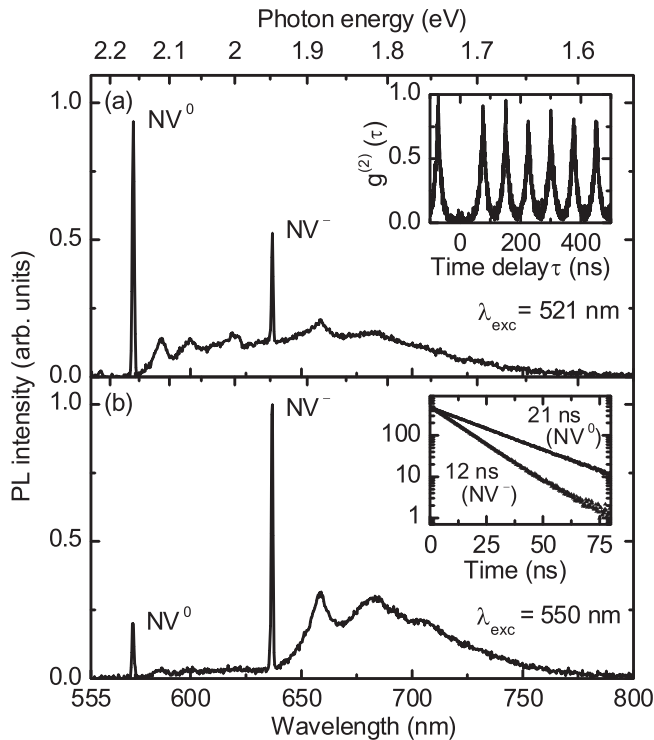


FIG. 1. Spectral and temporal analysis of the PL emission from an individual nitrogen-vacancy center at a temperature of $T = 10$ K. PL spectra are measured under excitation at a wavelength of (a) 521 and (b) 550 nm. The second-order photon correlation function $g^{(2)}(\tau)$ is shown in the inset of (a). The temporal PL decay for NV^0 and NV^- is depicted in the inset of (b).

PLE spectra of a single color center have been assembled in Fig. 2 by plotting the PL intensity of its negative (red circles) and neutral (blue triangles) state versus the excitation wavelength. If possible, we have evaluated the intensities of the ZPLs exclusively (filled symbols in Fig. 2). When λ_{exc} is close to one of the ZPLs at $T = 10$ K or generally at $T = 300$ K, we plot the peak intensities of the PSBs with proper rescaling (empty symbols in Fig. 2). The excitation power of $50 \mu\text{W}$ is kept well below saturation ($300 \mu\text{W}$). For a precise measurement of the unexpected sharp line in the PLE spectrum of NV^- at $\lambda_{\text{exc}} = 575$ nm (red trace in Fig. 2), we reduce the bandwidth of the tunable laser to 0.1 nm via a diffraction grating and spatial filter.

We now turn to a detailed analysis of the PLE spectrum from NV^- . To a first approximation, PLE and PL spectra of a vibronic quantum emitter are mirror symmetric relative to the ZPL. Interestingly, previous ensemble studies [16] meet this expectation, whereas our measurement on a single NV^- center does not (Fig. 2). Remarkably, no PL is detected at excitation wavelengths $\lambda_{\text{exc}} > 575$ nm. This phenomenon has been interpreted as a fast switching to a dark state, which was initially identified as a metastable singlet level [17] and more recently as a differently charged state of NV [12]. We now repeat our PLE measurement of

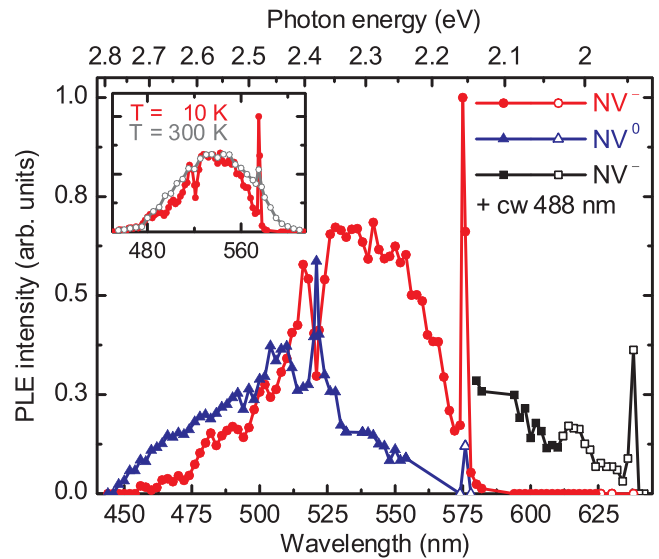


FIG. 2 (color). PLE spectra of NV^- (red circles), NV^- with an additional repump laser at 488 nm (black squares), and NV^0 (blue triangles) of an individual center at $T = 10$ K. The inset compares PLE spectra of single NV^- at $T = 300$ K (gray) and $T = 10$ K (red). In all traces filled and open symbols correspond to ZPL and rescaled PSB intensities, respectively.

NV^- under the presence of an additional “repump” laser [17] of a low cw power of $5 \mu\text{W}$ at 488 nm (black squares in Fig. 2). This laser produces weak PL by itself. However, efficient luminescence is observed in the two-color scheme for the entire interval from the ZPL of NV^- down to $\lambda_{\text{exc}} = 575$ nm. For excitation wavelengths $\lambda_{\text{exc}} < 575$ nm, the presence of the repump laser does not modify the PL of the NV center noticeably. Very surprisingly, in this region we recover distinct features expected for the absorption of NV^0 in the PLE spectrum of NV^- (red trace in Fig. 2): there is a sharp peak at a wavelength of 575 nm which corresponds exactly to the ZPL of NV^0 (Fig. 1). A broadband maximum follows at shorter wavelengths reminiscent of the anti-Stokes PSB.

Our physical interpretation of the unexpected spectral shape of the PLE of NV^- is as follows [schematic illustration in Fig. 3(a)]: NV^- absorption starts with a sharp ZPL at 637 nm and continues down to approximately 450 nm in form of a broad PSB [18]. The absorption of NV^0 looks similar, but is spectrally blueshifted into the range between 575 nm (ZPL) and roughly 400 nm [19]. Laser optical excitation of a single center produces photo-induced charge switching between NV^0 and NV^- in both directions. The $NV^- \rightarrow NV^0$ process proceeds exclusively from the excited state of NV^- [15]. Our observation that the PLE spectrum of NV^- is modulated with the absorption spectrum of NV^0 implies that the reverse process $NV^0 \rightarrow NV^-$ happens similarly, only from the excited state of NV^0 . These occasional charge conversions can be illustrated by the schematic loop in Fig. 3(a)

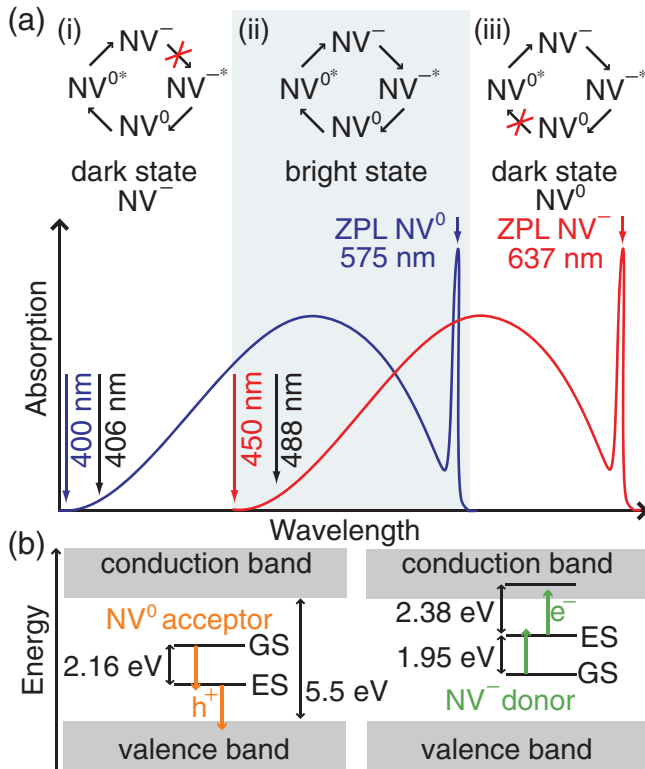


FIG. 3 (color). (a) Schematic representation of the low-temperature absorption spectra of NV⁻ (red) and NV⁰ (blue) together with relevant switching cycles (top). Red crosses denote breaks in the recharging cascade. The gray shaded region (ii) corresponds to the joint absorption of both charge states, where continuous charge switching (stars denote excited states) and therefore efficient NV luminescence is possible. (b) Simplified electronic energy schemes of the nitrogen-vacancy center. The optical transition from ground state (GS) to excited state (ES) is followed either by an excitation of an electron (e^-) into the conduction band (green arrows) for NV⁻ (right) or an excitation of a hole (h^+) into the valence band (orange arrows) for NV⁰ (left). An additional electronic resonance of NV⁻ is located in the conduction band of diamond.

(stars denote electronic excited states). When exciting in the wavelength band from 450 to 575 nm [region (ii), gray shaded] where both NV⁰ and NV⁻ absorb efficiently, the loop is closed and temporal averaging results in a combination of both PL bands (Fig. 1). However, if only NV⁻ is excited [$575 \text{ nm} < \lambda_{\text{exc}} < 637 \text{ nm}$, region (iii)], the loop is broken. The first photoinduced switch rapidly transfers the center into its long lived and nonabsorbing neutral state. This situation does not produce PL and switching back to the absorbing variant is inhibited. Consequently, NV⁰ is effectively the dark state of NV⁻. Additional low-power radiation at 488 nm efficiently excites NV⁰ [Fig. 3(a)] and drives the NV⁰ \rightarrow NV⁻ process (repumping).

Vice versa, the excitation of only NV⁰ with a cw laser at 406 nm produces no PL, as expected, since the loop is disrupted due to the lack of the NV⁻ absorption in region (i). The two-color scheme with one laser exciting solely

NV⁻ and another exclusively NV⁰ corresponds again to the closed loop. We verify this effect by simultaneous application of the laser at $\lambda_{\text{exc}} = 406 \text{ nm}$ and the tunable one with $575 \text{ nm} < \lambda_{\text{exc}} < 637 \text{ nm}$. In perfect agreement with our model, we then observe stable PL of both charge variants of NV, although neither one of these lasers alone induces emission.

As a consequence of the requirement for electronic excitation in order to switch between charge states, the effective PLE spectra of both NV⁻ and NV⁰ are essentially the product of their absorption profiles and thus confined to the wavelength region from 450 to 575 nm. The products have to be weighted with additional factors depending mainly on the conversion rates (compare quantitative differences between red and blue graphs in Fig. 2). Note that at $T = 300 \text{ K}$ (inset in Fig. 2), some spectral weight is recovered in the PLE spectrum of NV⁻ at $\lambda_{\text{exc}} > 575 \text{ nm}$. This behavior is expected in our model because of the extension of NV⁰ absorption due to the thermal occupation of phonons in the electronic ground state.

The present understanding of the NV⁰ \rightarrow NV⁻ conversion is as follows: Optical excitation of an electron from a substitutional N atom into the conduction band of diamond is followed by its capture by NV⁰ [11]. The energy threshold of electron excitation from a N donor is supposed to fall somewhere between 2.33 eV (532 nm) and 1.95 eV (637 nm), since excitation at 532 nm activates the conversion, whereas pumping at 637 nm does not [11]. However, we find no feature in the PLE spectra which may be assigned to the ionization of N donors. In addition, the current model does not require the optical excitation of NV⁰.

Our new findings motivate an alternative and intrinsic origin of the NV⁰ \rightarrow NV⁻ conversion in complete analogy with the reverse process [Fig. 3(b)]. It is accepted that the NV⁻ \rightarrow NV⁰ transition occurs in two steps [15] (green arrows): First, the optical transition of NV from ground state (GS) to excited state (ES) [20] and second, the excitation of an electron into the conduction band of the diamond host lattice. We now suggest that switching from NV⁰ to NV⁻ proceeds via the GS to ES transition, followed by transferring a hole into the valence band (orange arrows). In Fig. 3(b) NV⁻ is shown as an electron donor (right) and NV⁰ as an electron acceptor (left, reversed level order). The single-step charge conversions are inhibited due to the requirement of higher photon energy.

We suspect that earlier PLE studies investigating ensembles of NVs did not reveal the charge switching effects due to the weak intensity from thermal excitation sources [18,19]. In order to support this hypothesis, we repeat the PLE experiment at low temperature in a chemical vapor deposition sample which is still relatively pure (concentration of N atoms $< 1 \text{ ppm}$, ~ 5000 NV centers in the confocal volume). The PLE spectra are similar to those in Fig. 2 (not shown), except for excitation wavelengths $\lambda_{\text{exc}} > 575 \text{ nm}$. Here, the PL signal of NV⁻ does not vanish

immediately but decays on a time scale of 10 minutes and saturates at a finite value. This behavior is expected in our analysis: NV^- defects in the center of the confocal volume switch into the dark state rapidly, their neighbors out of focus transform more slowly, and the weakly excited specimens in the periphery of the spot never lose their extra electron. The PL of the latter centers is well detectable due to the summation over a large ensemble. A weak excitation in the joint absorption region of NV^0 and NV^- restores the initial PL intensity measured at $\lambda_{\text{exc}} > 575$ nm since it activates the $NV^0 \rightarrow NV^-$ switching. Interestingly, leaving the sample without optical irradiation for several minutes does not change the PL level observed previously. This finding confirms the purely photoinduced nature of both charge switching processes.

A full understanding of the switching dynamics between NV^- and its undesirable dark state (NV^0) is achieved by summarizing our observations together with previous findings [12,17]. Under nonresonant optical excitation close to saturation, switching occurs on the submicrosecond time scale [12]. We estimate the average dwell time of the center in Fig. 2 in its neutral state from the ratio of the strengths of NV^- and NV^0 emission, taking into account the difference in PL lifetimes. Our value of 17% at $\lambda_{\text{exc}} = 532$ nm is in good agreement with the 30% reported previously [12]. We find that the dwell time is independent of laser power over a wide interval between 2% and 200% of the saturation value. Consequently, the photoconversion rates between NV^0 and NV^- should exhibit the same intensity dependence. This behavior was reported to be quadratic for both processes [12], thus further supporting our two-step switching model [Fig. 3(b)].

At low temperature, a wavelength of 575 nm excites the NV^- center most efficiently (Fig. 2) since fortunately the broad absorption maximum of the PSB of NV^- [18] coincides with the ZPL of NV^0 [19]. This observation is vital, e.g., for the generation of indistinguishable photons with NV^- because for excitation at 575 nm less power is needed compared to conventional pumping at 532 nm and the photon energy is lower. As a consequence, less unwanted charge fluctuations should result due to the ionization of impurities in the vicinity of a center and thus there will be less spectral jumps and spectral diffusion.

Another interesting observation in the PLE spectra of NV is the sharp feature at 521 nm (2.38 eV) (Fig. 2). We assign this phenomenon to an electronic transition of NV^- out of its ES at 1.95 eV to a level located 2.38 eV higher in energy in the conduction band of the diamond host lattice [Fig. 3(b)]. Remarkably, the energy of the extra level relative to the GS of NV^- is equal to 4.33 eV. It corresponds exactly to an absorption line in diamond at 4.325 eV which correlates with the NV^- concentration [21]. Because of the rapid decay with the release of an electron into the conduction band, no PL is expected from the 4.33 eV state. Indeed, the excitation with

$\lambda_{\text{exc}} < 500$ nm does not produce a corresponding ZPL at 521 nm in the PL spectra of NV. The efficient loss of the electron leads to a peak (dip) in the PLE spectrum of NV^0 (NV^-). Close inspection of the narrow feature around 521 nm in the PLE spectrum of NV^0 in Fig. 2 suggests a Fano-type line shape [22] which is typical for a discrete resonance coupled to a broadband continuum. The asymmetry is less obvious in the PLE spectrum of NV^- due to the overlap with the steep PSB background.

Not every individual NV shows the resonance at 521 nm (observed for 18 out of 30 centers), whereas its presence correlates with the PL lifetime of NV^- . The feature is observable for decay times between 10.1 and 12.1 ns and absent for shorter lifetimes between 9.8 and 10.0 ns (measurement accuracy: ± 0.1 ns). The lifetime of NV^0 of 20.7 ± 0.6 ns does not vary noticeably. The random local strain of the diamond host crystal can modify the decay channels of NV^- [23], resulting in a variation of optical spin polarization and population of the 1.95 eV ES sub-levels. We expect the shortening of the NV^- PL lifetime along with the quenching of the transition to the 4.33 eV state to be a consequence of this effect. Note that the excitation of the selected centers at 521 nm efficiently converts them into the neutral form which can be exploited for optimized single-photon sources based on NV^0 .

In summary, we report a strong and unexpected dependence of the PL emission of single NV centers in ultrapure diamond on the excitation wavelength. The ubiquitous dark state [12,17], assigned to NV^0 , is optimally repumped back to NV^- at 575 nm. Pumping at 521 nm efficiently converts the centers to their neutral state. These results are crucial for numerous applications of NV centers, whenever optimum absorption efficiency, cleanness of emission, and/or minimum spurious excitation are required.

The authors would like to thank Johannes Haase, Tobias Hanke, and Petr Siyushev for stimulating discussions.

*Corresponding author

anton.batalov@uni-konstanz.de

†Present address: Chemnitz University of Technology, Institute of Physics, D-09107 Chemnitz, Germany.

- [1] T. Gaebel *et al.*, *Nature Phys.* **2**, 408 (2006).
- [2] G.D. Fuchs, G. Burkard, P.V. Klimov, and D.D. Awschalom, *Nature Phys.* **7**, 789 (2011).
- [3] B.B. Buckley, G.D. Fuchs, L.C. Bassett, and D.D. Awschalom, *Science* **330**, 1212 (2010).
- [4] E. Togan *et al.*, *Nature (London)* **466**, 730 (2010).
- [5] J.R. Maze *et al.*, *Nature (London)* **455**, 644 (2008).
- [6] G. Balasubramanian *et al.*, *Nature (London)* **455**, 648 (2008).
- [7] C. Kurtsiefer, S. Mayer, P. Zarda, and H. Weinfurter, *Phys. Rev. Lett.* **85**, 290 (2000).
- [8] A. Beveratos, R. Brouri, T. Gacoin, A. Villing, J.-P. Poizat, and P. Grangier, *Phys. Rev. Lett.* **89**, 187901 (2002).

- [9] C. K. Hong, Z. Y. Ou, and L. Mandel, *Phys. Rev. Lett.* **59**, 2044 (1987).
- [10] D. L. Moehring, P. Maunz, S. Olmschenk, K. C. Younge, D. N. Matsukevich, L.-M. Duan, and C. Monroe, *Nature (London)* **449**, 68 (2007).
- [11] L. Robledo, H. Bernien, I. van Weperen, and R. Hanson, *Phys. Rev. Lett.* **105**, 177403 (2010).
- [12] G. Waldherr, J. Beck, M. Steiner, P. Neumann, A. Gali, Th. Frauenheim, F. Jelezko, and J. Wrachtrup, *Phys. Rev. Lett.* **106**, 157601 (2011).
- [13] V. Zwiller and G. Björk, *J. Appl. Phys.* **92**, 660 (2002).
- [14] K. Moutzouris, F. Adler, F. Sotier, D. Träutlein, and A. Leitenstorfer, *Opt. Lett.* **31**, 1148 (2006).
- [15] N. B. Manson and J. P. Harrison, *Diamond Relat. Mater.* **14**, 1705 (2005).
- [16] H. Hanzawa, H. Nishikori, Y. Nisida, S. Sato, T. Nakashima, S. Sasaki, and N. Miura, *Physica (Amsterdam)* **184B**, 137 (1993).
- [17] K. Y. Han, S. K. Kim, C. Eggeling, and S. W. Hell, *Nano Lett.* **10**, 3199 (2010).
- [18] G. Davies and M. F. Hamer, *Proc. R. Soc. A* **348**, 285 (1976).
- [19] G. Davies, *J. Phys. C* **12**, 2551 (1979).
- [20] J. R. Weber, W. F. Koehl, J. B. Varley, A. Janotti, B. B. Buckley, C. G. Van de Walle, and D. D. Awschalom, *Proc. Natl. Acad. Sci. U.S.A.* **107**, 8513 (2010).
- [21] I. N. Kupriyanov, V. A. Gusev, Yu. N. Pal'yanov, and Yu. M. Borzdov, *J. Phys. Condens. Matter* **12**, 7843 (2000).
- [22] U. Fano, *Phys. Rev.* **124**, 1866 (1961).
- [23] A. Batalov, V. Jacques, F. Kaiser, P. Siyushev, P. Neumann, L. J. Rogers, R. L. McMurtrie, N. B. Manson, F. Jelezko, and J. Wrachtrup, *Phys. Rev. Lett.* **102**, 195506 (2009).